Multimode quantitative scanning microwave microscopy of *in situ* grown epitaxial $\mathrm{Ba_{1-x}Sr_xTiO_3}$ composition spreads

K. S. Chang, M. Aronova, O. Famodu, and I. Takeuchi[a)]
Department of Materials Science and Engineering, and Center for Superconductivity Research, Department of Physics, University of Maryland, College Park, Maryland 20742

S. E. Lofland[b)] and J. Hattrick-Simpers
Department of Physics and Chemistry, Rowan University, Glassboro, New Jersey 08028

H. Chang
Materials Sciences Division, Lawrence Berkeley National Laboratory, Berkeley, California 94720

(Received 17 August 2001; accepted for publication 10 October 2001)

We have performed variable-temperature multimode quantitative microwave microscopy of *in situ* epitaxial $\mathrm{Ba_{1-x}Sr_xTiO_3}$ thin-film composition spreads fabricated on (100) LaA1O$_3$ substrates. Dielectric properties were mapped as a function of continuously varying composition from BaTiO$_3$ to SrTiO$_3$. We have demonstrated nondestructive temperature-dependent dielectric characterization of local thin-film regions. Measurements are simultaneously taken at multiple resonant frequencies of the microscope cavity. The multimode measurements allow frequency dispersion studies. We observe strong composition-dependent dielectric relaxation in $\mathrm{Ba_{1-x}Sr_xTiO_3}$ at microwave frequencies. © *2001 American Institute of Physics.* [DOI: 10.1063/1.1427438]

Microwave near-field microscopy is a powerful technique for quickly obtaining spatially resolved electrical impedance information on a variety of samples.[1–4] In particular, properties of ferroelectric/dielectric materials are widely being investigated using microwave microscopy.[4–6] Quantitative microwave dielectric characterization of thin films using the microscope has been previously demonstrated.[4,7–9]

The microscopes are ideal tools for rapid characterization and mapping of combinatorial libraries and composition spreads.[10,11] They have been used to screen combinatorial libraries of $\mathrm{Ba_{1-x}Sr_xTiO_3}$ (BST) and related materials systems. These studies have been fruitful in identifying compositions with improved dielectric properties. Combinatorial investigations are also effective in systematically studying the underlying physics of materials.[12]

Recognizing that optimized materials properties exist in a multidimensional parameter space, it is desirable to be able to map the properties of materials not just as a function of composition, but also as functions of other parameters such as temperature and measurement frequency at the same time. It is expected that such a comprehensive characterization strategy will become increasingly more important in future combinatorial and other rapid materials investigations.

We report here on variable-temperature multifrequency quantitative microwave microscopy of in situ deposited epitaxial BST spreads. We have mapped the complex dielectric constant of the spread as a function of frequency and temperature. We observe a systematic dispersion effect, which depends strongly on the composition. We attribute this to high-frequency relaxation, which arises from coupling of the microwave field to the phonon soft mode.

For fabricating the spread, we have used our combinatorial pulsed laser deposition (PLD) system. Two ceramic targets, BaTiO$_3$ (BTO) and SrTiO$_3$ (STO), were ablated in an alternating manner with an excimer laser (KrF with $\lambda = 248$ nm) for deposition onto a (100) LaA1O$_3$ substrate. Linear compositional gradient across the spread is created by performing a series of shadow depositions through a rectangular opening in an automated shutter, which moves back and forth over the substrate during the deposition. The typical distance between the shutter plane and the substrates is 300 μm. The motion of the shutter is synchronized with the firing of the laser in such a way so that for each deposition, a thickness gradient ''wedge'' is created on a chip. In order to ensure alloy-like intermixing of BTO and STO at the atomic level, less than a unit cell ($\approx$0.4 nm) is deposited for each set of BTO/STO deposition at any position on the spread. This is shown schematically in the lower inset of Fig. 1. The resulting spread has the composition varying continuously from

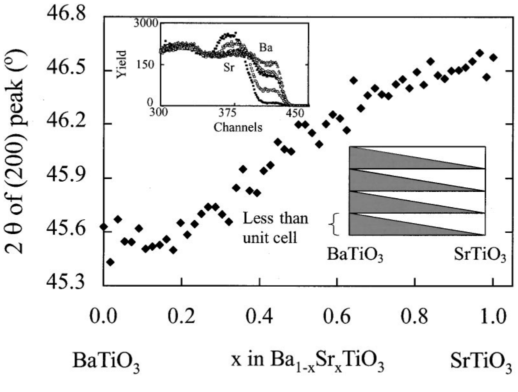

FIG. 1. 2θ value of the (200) peak vs composition on a $\mathrm{Ba_{1-x}Sr_xTiO_3}$ spread. Continuous change in the value is observed from 45.4° for BaTiO$_3$ to 46.5° for SrTiO$_3$. The upper inset shows Ba and Sr regions of selected RBS taken at different positions on the spread. A systematic shift in the spectra is seen. The lower inset shows the deposition scheme for the spread.

[a)] Electronic mail: takeuchi@squid.umd.edu

[b)] Also at: Department of Physics, University of Maryland, College Park, MD 20742.

0003-6951/2001/79(26)/4411/3/$18.00

© 2001 American Institute of Physics
Downloaded 17 Jun 2008 to 129.2.175.79. Redistribution subject to AIP license or copyright; see http://apl.aip.org/apl/copyright.jsp

pure BTO at one end to pure STO at the other end. The deposition substrate temperature was 800 °C, and the oxygen partial pressure was 100 mTorr. The ablation energy was approximately 2 J/cm^2, and the total thickness at each position on the spread was ≈200 nm. The sample was approximately 6 mm long in the spread direction.

A scanning x-ray microdiffractometer (D8 DISCOVER with GADDS for combinatorial screening by Bruker-AXS) was used to characterize the out-of-plane lattice constant of the film across the spread chip. Figure 1 shows the observed 2θ values of the (200) diffraction peak versus the intended composition on the spread. This particular measurement was taken with a 50-μm-diam. x-ray beam. The continuous lattice parameter change is evident, and the 2θ values obtained at various compositions are in good agreement with reported values.[13] We have also used Rutherford backscattering spectroscopy (RBS) to confirm the composition of the spread. The upper inset of Fig. 1 shows Ba and Sr peak regions of selected RBS spectra from various spots on the spread.

High-resolution cross-sectional transmission electron microscopy (TEM) of a single-composition $Ba_{0.3}Sr_{0.7}TiO_3$ film made in a similar way as described above indicated that the films are epitaxial with atomically sharp interfaces with the substrates.[14] The TEM measurements also revealed a high density of threading dislocations, a common feature for epitaxial BST films deposited on substrates with small lattice mismatch.[15]

A scanning microwave near-field evanescent microscope is used for dielectric characterization of the BST composition spread at microwave frequencies. The microscope consists of a high-*Q* λ/4 coaxial cavity with a scanning tunneling microscope tip mounted to the center conductor, which protrudes through an aperture in the bottom plate.[1] A network analyzer (HP8720C) allows us to make simultaneous multimode measurements using higher harmonics of the fundamental cavity mode, which is at 0.95 GHz. The typical *Q* value is 2000. The multimode measurements are crucial for frequency dispersion studies of materials. A simple coil heater is mounted to the sample stage, which allows us to perform variable-temperature measurements between room temperature and ≈ 200 °C. A numerical algorithm converts the extracted values of shifts in the resonant frequencies and *Q* of the resonator to obtain quantitative values of complex dielectric constants of a sample placed underneath the tip.[4]

Measurements were taken on the spread at different positions as the tip is scanned over the spread, so that data are collected as a function of composition. Figure 2 shows the composition-spread profile of the dielectric constant at three different frequencies measured simultaneously at room temperature. The profile shows a continuous change with the expected compositional dependence: the peak in the profile is located near $Ba_{0.65}Sr_{0.35}TiO_3$, which has its Curie temperature near room temperature. On either side of this composition, the dielectric constant is lower. The inset shows the loss tangent profile at 0.95 GHz. The loss tangent increases with decreasing value of *x* in the composition. The dielectric constant and loss values observed here are similar to the values reported in similar microscope measurements taken on single-composition BST films.[16] The overall compositional dependence seen here is qualitatively similar to that typically observed at much lower frequencies (<1 MHz).

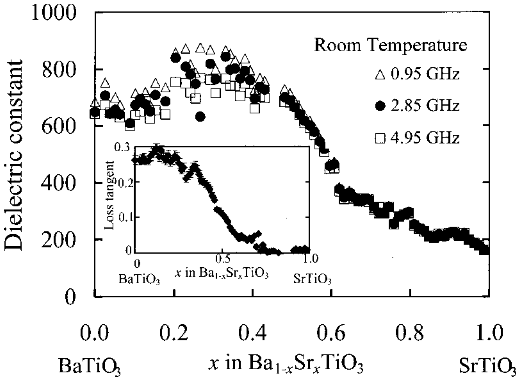

FIG. 2. Dielectric constant vs composition on a spread measured at 0.95, 2.85, and 4.95 GHz at room temperature. The highest dielectric constant occurs at $Ba_{0.65}Sr_{0.35}TiO_3$. The inset shows the spread profile of the loss tangent at 0.95 GHz at room temperature.

We have studied the temperature dependence of the spread profile of the dielectric constant. Compared to the room-temperature profile, profiles at higher temperatures display a shift in the highest dielectric constant composition toward lower *x* compositions as expected from the systematic variation in the Curie temperature. Figure 3 shows the spread profile at 0.95 GHz at room temperature and at 130 °C. The peak at 130 °C is at $Ba_{0.8}Sr_{0.2}TiO_3$ whose bulk Curie point is near that temperature. The inset shows the temperature dependence of the dielectric constant taken while the position of the microscope tip was held fixed over a position on the spread where the composition is $Ba_{0.75}Sr_{0.25}TiO_3$. The broad maximum in the dielectric constant is typical of BST thin films.[13]

One central issue in BST films is the presence of frequency dispersion in their dielectric properties. The existence of frequency dispersion can seriously undermine their application. To date, there are a limited number of systematic studies of high-frequency dispersion in BST films. Dispersive behavior at microwave frequencies has been reported in epitaxial STO films at low temperatures[17] and BST films grown on semiconductor substrates.[18,19] Recently, Hubert and Levy have used a local dynamical optical probe to reveal the existence of mesoscopic microwave dispersion in epitaxial BST films.[20]

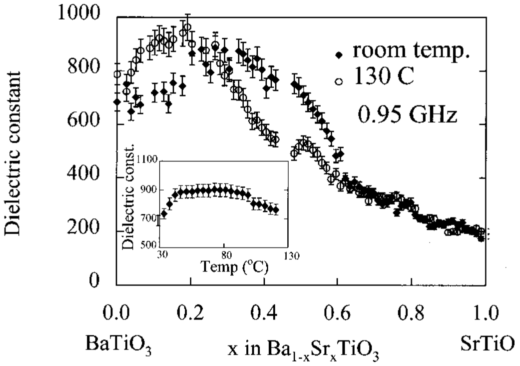

FIG. 3. Dielectric constant vs composition on a spread at room temperature and at 130 °C. The composition with highest dielectric constant value shifts toward the Ba-rich side as the temperature is increased. The inset shows the temperature dependence of the dielectric constant for $Ba_{0.65}Sr_{0.35}TiO_3$.

Downloaded 17 Jun 2008 to 129.2.175.79. Redistribution subject to AIP license or copyright; see http://apl.aip.org/apl/copyright.jsp

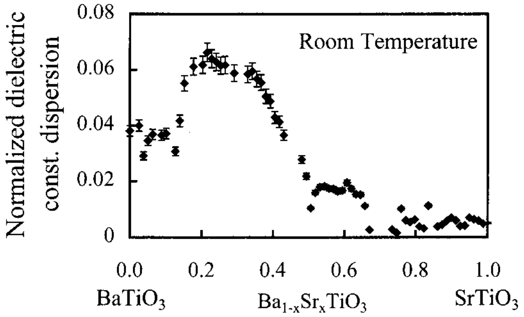

FIG. 4. Normalized dielectric constant dispersion defined as $(\epsilon_{0.95\,\mathrm{GHz}}-\epsilon_{4.95\,\mathrm{GHz}})/\epsilon_{0.95\,\mathrm{GHz}}$ vs composition on a spread at room temperature. The largest dielectric dispersion occurs at $x=0.2-0.4$.

From Fig. 2, it is evident that the dielectric constant tends to decrease as the measurement frequency is increased for compositions with a high Ba/Sr ratio. To illustrate this more clearly, we plot the spread profile of the normalized dielectric constant dispersion at room temperature in Fig. 4. Here, we define the normalized dielectric constant dispersion to be the difference in the measured dielectric constant between 0.95 and 4.95 GHz from the data in Fig. 2 divided by the dielectric constant at 0.95 GHz. A pronounced compositional-dependent effect similar to the one seen in Fig. 2 is observed. The dispersion is minimal or close to zero near the STO end of the spread. It increases with increasing Ba content, reaches the highest values for x at around 0.2–0.4, and decreases again as x approaches zero. The observed dispersion here directly points to the presence of strong dielectric relaxation, and it is closely tied to the onset of ferroelectricity. It is largest for compositions experiencing the ferroelectric transitions. Above and below the transition temperature, the dispersion is reduced. When the measurement temperature is increased, the dielectric dispersion peak was seen to move toward compositions with higher Ba concentration (not shown), mirroring the shift in maximum of the dielectric constant.

It is known that phonon mechanisms can give rise to dielectric losses at microwave frequencies.[21] We believe that the observed relaxation behavior is a result of interaction of the phonon soft mode with electromagnetic excitation in the film.[22] The role of the soft mode in the dielectric properties of STO films has been previously elucidated.[23] Coupling of the microwave field with the local soft mode may be mediated by the presence of structural defects such as threading dislocations. The soft-mode frequencies are in the THz range, but depending on the nature of the interaction, it can result in loss and relaxation that have a very broad frequency distribution (stretching from the GHz to THz range).[21,22] As the soft mode undergoes softening/hardening, there is an accompanied overall shift in the relaxation range. Such a shift to a lower-frequency range results in increased dielectric dispersion at 1–5 GHz. The observed compositional dependence of the dispersion (Fig. 4) is entirely consistent with the behavior of the soft mode near a paraelectric–ferroelectric transition, where the mode undergoes significant softening.[24] The dielectric frequency dispersion is maximum near the compositions undergoing transition, and above and below the transition range, it is markedly lower. In the spread profile, above and below the transition temperature "correspond" to the composition regions to the right of the "hump" and the left of the "hump" in Fig. 4, respectively. Thus, a single temperature measurement of the composition spread here allows an indirect probe of the temperature-dependent behavior of the entire BST system.

The authors acknowledge J. C. Booth for useful discussions, Beth Nechkash for taking the x-ray data, and R. P. Sharma for the RBS measurements. This work was supported by NSF Grant No. DMR 0094265 (CARREER) and DMR 0076456 and partially supported by NSF Grant No. MRSEC DMR-80008.

[1] T. Wei, X.-D. Xiang, W. G. Wallace-Freedman, and P. G. Schultz, Appl. Phys. Lett. **68**, 3506 (1996).
[2] I. Takeuchi, T. Wei, F. Duewer, Y. K. Yoo, X.-D. Xiang, V. Talyansky, S. P. Pai, G. J. Chen, and T. Venkatesan, Appl. Phys. Lett. **71**, 2026 (1997).
[3] A. F. Lann, M. Golosovsky, D. Davidov, and A. Frenkel, Appl. Phys. Lett. **73**, 2832 (1998).
[4] C. Gao and X.-D. Xiang, Rev. Sci. Instrum. **69**, 3846 (1998).
[5] Y. Lu, T. Wei, F. Duewer, Y. Lu, N. B. Ming, P. G. Schultz, and X.-D. Xiang, Science **276**, 2004 (1997).
[6] D. E. Steinhauer, C. P. Vlahacos, F. C. Wellstood, S. M. Anlage, C. Canedy, R. Ramesh, A. Stainishevsky, and J. Melngailis, Appl. Phys. Lett. **75**, 3180 (1999).
[7] J. H. Lee, S. Hyun, and K. Char, Rev. Sci. Instrum. **72**, 1425 (2001).
[8] Y. G. Wang, M. E. Reeves, and F. S. Rachford, Appl. Phys. Lett. **76**, 3295 (2000).
[9] Y. Cho, S. Kazuta, and K. Matsuura, Appl. Phys. Lett. **75**, 2833 (1999).
[10] H. Chang, C. Gao, I. Takeuchi, Y. Yoo, J. Wang, P. G. Schultz, X.-D. Xiang, R. P. Sharma, M. Downes, and T. Venkatesan, Appl. Phys. Lett. **72**, 2185 (1998).
[11] H. Chang, I. Takeuchi, and X.-D. Xiang, Appl. Phys. Lett. **74**, 1165 (1999).
[12] T. Fukumura, M. Ohtani, M. Kawasaki, Y. Okimoto, T. Kageyama, T. Koida, T. Hasegawa, Y. Tokura, and H. Koinuma, Appl. Phys. Lett. **77**, 3426 (2999).
[13] Y. Gim, T. Hudson, Y. Fan, C. Kwon, A. Findikoglu, B. J. Gibbons, B. H. Park, and Q. X. Jia, Appl. Phys. Lett. **77**, 1200 (2000).
[14] L. A. Bendersky, C. J. Lu, K. S. Chang, and I. Takeuchi (unpublished).
[15] C. L. Canedy, Hao Li, S. P. Alpay, L. Salamanca-Riba, A. L. Roytburd, and R. Ramesh, Appl. Phys. Lett. **77**, 1695 (2000).
[16] Y. G. Wang, M. E. Reeves, W. J. Kim, J. S. Horwitz, and F. J. Rachford, Appl. Phys. Lett. **78**, 3872 (2001).
[17] M. J. Dalberth, R. E. Stauber, J. C. Price, C. T. Rogers, and D. Galt, Appl. Phys. Lett. **72**, 507 (1998).
[18] R. Jammy and L. A. Wills, Integr. Ferroelectr. **15**, 235 (1997).
[19] K. Ikuta, Y. Umeda, and Y. Ishii, Jpn. J. Appl. Phys., Part 2 **34**, L1211 (1995).
[20] C. Hubert and J. Levy, Phys. Rev. Lett. **85**, 1998 (2000).
[21] A. Tagantsev, Mater. Res. Soc. Symp. Proc. **603**, 221 (2000).
[22] J. C. Booth, R. H. Ono, I. Takeuchi, and K.-S. Chang (unpublished).
[23] A. A. Sirenko, C. Bernhard, A. Golnik, A. M. Clark, J. Hao, W. Si, and X. X. Xi, Nature (London) **404**, 373 (2000); I. A. Akimov, A. A. Sirenko, A. M. Clark, J.-H. Hao, and X. X. Xi, Phys. Rev. Lett. **84**, 4625 (2000).
[24] M. E. Lines and A. M. Glass, *Principles and Applications of Ferroelectrics and Related Materials* (Oxford University Press, New York, 1977).

Downloaded 17 Jun 2008 to 129.2.175.79. Redistribution subject to AIP license or copyright; see http://apl.aip.org/apl/copyright.jsp